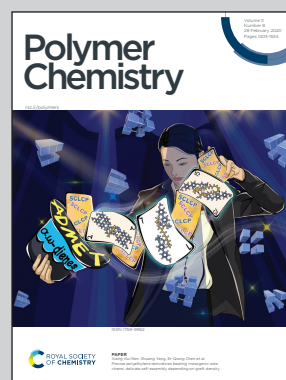


**Highlighting research output from Rajiv Gandhi Institute of Petroleum Technology, Jais, India.**

Solvent processable and recyclable covalent adaptable organogels based on dynamic trans-esterification chemistry: separation of toluene from azeotropic mixtures

Umaprasana Ojha and coworkers have developed a set of covalent adaptive organogels based on dynamic ester linkages which can be solution processed with retention of mechanical properties and recycled back to the precursors. These organogels are capable of selectively absorbing aromatics compared to a range of other common organic solvents and may be utilized to separate aromatics from azeotropic mixtures.

**As featured in:**






See Umaprasana Ojha *et al.*,  
*Polym. Chem.*, 2020, **11**, 1471.

## PAPER

[View Article Online](#)  
[View Journal](#) | [View Issue](#)Cite this: *Polym. Chem.*, 2020, **11**, 1471

# Solvent processable and recyclable covalent adaptable organogels based on dynamic trans-esterification chemistry: separation of toluene from azeotropic mixtures†

Suman Debnath,  Swaraj Kaushal,  Subhankar Mandal  and Umaprasana Ojha \*

New covalent adaptable networks (CANs) possessing processability and recyclability to monomers are desirable as an alternative to traditional plastics to address plastic waste-related issues. Moreover, conventional polymeric networks are generally insoluble in organic solvents. Herein, we report a set of CANs that can be dissolved in alcoholic solvents *via* reactive depolymerization and fully recycled to monomers. In this study, we have utilized trans-esterification of  $\alpha$ -substituted  $\beta,\beta'$ -diesters with multi-hydroxy compounds under moderate temperature conditions (110–140 °C) to develop a set of polyester-based CANs. The synthesized CANs showed ultimate tensile strength (UTS) and elongation at break values up to ~1.1 MPa and ~595%, respectively. These CANs showed thermal stability up to 215 °C. The films were stable under acidic and basic conditions. These CANs readily depolymerized and dissolved in an alcoholic solvent at ~120 °C within 15 h *via* competitive trans-esterification with the solvent. The films re-formed on evaporation of the solvent followed by curing at 140 °C. The reprocessed CANs exhibited UTS (~1.0 MPa) and Young's modulus (~1.8 MPa) values comparable to the original samples. Due to their simple synthesis, solvent processability, recyclability, economically reliable starting materials and moderate processing temperature, these polyester CANs may be suitable for various commercial applications. The CANs swiftly and selectively absorbed aromatic compounds compared to other organic solvents and swelled by ~750 wt% in toluene within 90 min. These properties were utilized to efficiently separate aromatics from various azeotropic mixtures involving toluene, methanol and water.

Received 28th November 2019,  
Accepted 29th January 2020

DOI: 10.1039/c9py01807g

[rsc.li/polymers](http://rsc.li/polymers)

## Introduction

Crosslinked polymeric networks possessing dynamic covalent linkages capable of undergoing a reversible exchange reaction in the presence of external stimuli are an important area of research in materials science.<sup>1,2</sup> These covalent adaptable networks (CANs) or dynamic covalent networks are able to match the mechanical properties,<sup>3</sup> thermal stability,<sup>4</sup> and solvent resistance<sup>5</sup> of conventional thermosets and overcome the associated nonprocessability issue.<sup>6</sup> Dynamic covalent linkages present in these CANs undergo swift exchange reaction when triggered by external stimuli such as temperature,<sup>7</sup> light,<sup>8</sup>

solvents<sup>9,10</sup> and reagents.<sup>11</sup> This enables a change in the topology of CANs and reprocessability of the samples under specific conditions.<sup>12</sup> Therefore, these CANs are favorable candidates for a range of applications including recyclable commodity plastics,<sup>13</sup> self-healing materials,<sup>14</sup> shape memory polymers,<sup>15,16</sup> reversible adhesives,<sup>17</sup> actuators,<sup>18</sup> and coatings.<sup>19</sup> Several functional linkages including Diels–Alder adducts,<sup>20</sup> imines,<sup>21</sup> Michael adducts,<sup>22</sup> amides,<sup>23</sup> hydrazones,<sup>24,25</sup> urethanes,<sup>26,27</sup> disulfide linkages,<sup>28</sup> vinyl-ogous urethanes,<sup>29</sup> carbonates,<sup>30</sup> and boronate esters<sup>31</sup> have been successfully studied as dynamic linkages in CANs. Some of the CANs have also shown the ability to recycle back to monomers under specific conditions.<sup>32</sup> Recyclability enables swift degradation of the CANs *via* depolymerization to the corresponding monomeric precursors.

Hydrogels and organogels based on dynamic covalent linkages are an important class of materials.<sup>33,34</sup> Such gel systems have exhibited self-healing ability,<sup>35</sup> responsiveness,<sup>36</sup> and dynamic control of the morphology<sup>37</sup> and are studied for their potential use in drug delivery matrices,<sup>38</sup> scaffolds for

Department of Chemistry, Rajiv Gandhi Institute of Petroleum Technology, Jais, Amethi, UP, 229304, India. E-mail: [uojha@rgipt.ac.in](mailto:uojha@rgipt.ac.in); Tel: +915352704510

† Electronic supplementary information (ESI) available: HRMS, NMR and FTIR spectra of model compounds, stress relaxation data, mechanical properties of the original and reprocessed films, molar composition, optimization of data, mechanical property data comparison of the original and reprocessed CANs, and the activation energy calculation procedure. See DOI: 10.1039/c9py01807g

polymerization,<sup>39</sup> stem cell culture,<sup>40</sup> injectable hydrogels,<sup>41</sup> strain sensors,<sup>42</sup> and burn wound healing.<sup>43</sup> Efforts have been made to tailor the stiffness of the hydrogels *via* controlling the crosslink using light as a stimulus.<sup>44,45</sup> Recently, small molecule-based stimuli-responsive reversible hydrogels have been developed based on amine–formaldehyde chemistry.<sup>46</sup> Therefore, the design of new organogel systems based on dynamic covalent linkages is desirable for various materials applications.

Among the several reported CANs, dynamic polyesters with a wide range of mechanical properties are one of the widely studied class of CANs due to their potential applications in several areas.<sup>47,48</sup> Typically, trans-esterification catalysts such as Zn(acac)<sub>2</sub>,<sup>49</sup> Sn(Oct)<sub>2</sub>,<sup>50</sup> and Brønsted acid<sup>51</sup> are utilized to improve the efficiency of the exchange reaction in these CANs. A range of precursors have been designed and utilized for the development of dynamic ester-based networks in the literature.<sup>52,53</sup> Recently, we have utilized  $\beta,\beta'$ -diesters as activated precursors to develop catalyst-free polyester vitrimers.<sup>54</sup> The  $\beta,\beta'$ -diesters possessing no substituents in the  $\alpha$  position reached trans-esterification equilibrium within 3 h at 100 °C in the presence of 5 mol% Sn(Oct)<sub>2</sub>. However, substituents at the  $\alpha$  position are necessary to increase the number of ester functionalities and enhance the versatility of the precursor. Furthermore, multi-functional ester precursors will enable the use of low molecular weight hydroxyl precursors and the development of fully recyclable polyester CANs.

In this report, we have studied the effect of  $\alpha$ -substitution on the rate of trans-esterification of  $\beta,\beta'$ -diesters using  $\alpha$ -alkyl substituted  $\beta,\beta'$ -diesters as model compounds and Sn(Oct)<sub>2</sub> as a trans-esterification catalyst under moderate temperature conditions. Subsequently, several CANs were designed and prepared utilizing the above trans-esterification reaction as the key reaction. The thermal and mechanical properties of the resulting CANs were analyzed. The solvent processability and recyclability of these CANs were evaluated. The swellability of these CANs in different organic solvents was evaluated and subsequently the CANs were utilized to separate aromatics from azeotropic mixtures under ambient conditions.

## Experimental

### Materials

$\alpha$ -Butyl diethylmalonate (BEM, TCI Chemicals, >99.0%), *n*-hexanol (Alfa Aesar, 98.0%), tin(II) 2-ethylhexanoate (Sn(Oct)<sub>2</sub>, TCI Chemicals, >85.0%), 1,6-dibromohexane (Avra Synthesis, 98.0%), diethyl malonate (DEM, SD Fine Chem, 98.0%), potassium carbonate anhydrous (Fisher Scientific, 99.0%), acetonitrile (Merck, 99.0%), ethyl acetate (Fisher Scientific, 98.0%), sodium sulphate anhydrous (Finar Chemicals, 99.0%), triethanolamine (TEA, SD Fine Chem, 99.0%), pentaerythritol (PTE, Himedia Laboratories, >98.0%), poly(tetramethylene oxide) diol (PTMO, Sigma-Aldrich,  $M_n \sim 2900$ ), *n*-butanol (Nice Chemicals, 99.0%), deionized water collected from a PURELAB Option-Q water purifier, *N,N*-dimethyl-

formamide (DMF, Spectrochem, 99.0%), dimethyl sulphoxide (DMSO, Fisher Scientific, 98.0%), toluene (Fisher Scientific, 99.5%), octanol (Merck, 99.0%), methanol (SD Fine Chem, 99.0%), acetone (Molychem, 99.0%), and CDCl<sub>3</sub> (Sigma-Aldrich, 99.8 atom% D) were used as received, unless otherwise stated.

### Characterization

A JEOL-400 YH NMR spectrometer was used to record <sup>1</sup>H and <sup>13</sup>C NMR spectra at a 25 °C probe temperature. FTIR spectra were acquired using a PerkinElmer Spectrum Two with a PIKE MIRacle single reflection horizontal ATR accessory. An Agilent Accurate-Mass Q-TOF LC/MS 6520 was used for recording ESI-HRMS mass spectra and the peaks were assigned *m/z* values (% of the base peak). The ultimate tensile strength (UTS) of polymer films was measured by using an H5KL, Tinius Olsen machine in generic tensile mode using rectangular film specimens with a width of  $\sim 5$  mm and a thickness of  $\sim 0.8$  mm. Tensile data were recorded at  $\sim 25$  °C with a 5.0 mm min<sup>-1</sup> machine speed. For representing the data, we have taken the average of three measurements. Young's moduli (*E*) were calculated from the linear region of tensile traces. Dynamic mechanical analysis (DMA) was performed on a DMA Q-800 TA instrument in tension mode using the 50 ASTM D4065-01 procedure. Stress relaxation experiments were conducted at a constant strain value of 0.5% in compression mode and data were collected after 10 min of reaching the equilibrium. After normalization of the modulus, the activation energy was calculated. The width and thickness of the rectangular specimen samples were  $\sim 5$  and  $\sim 1.5$  mm, respectively. Thermal gravimetric analysis (TGA) was carried out using a TGA PT1000 Linseis system under a N<sub>2</sub> atmosphere. For TGA, 15 mg of powdered samples were heated up to 700 °C at a 10 °C min<sup>-1</sup> ramp. A DSC 4000 PerkinElmer instrument was used for the recording of differential scanning calorimetry (DSC) data under a N<sub>2</sub> atmosphere (50 mL min<sup>-1</sup>). During measurement, a finely powdered sample was taken in aluminum foil and heated from 0 °C to 180 °C at a rate of 10 °C min<sup>-1</sup>. After cooling to 0 °C, the sample was again heated to 180 °C to obtain glass transition temperature (*T<sub>g</sub>*) values. For recording the ultraviolet-visible (UV-Vis) spectra, a UV-VIS 3200 instrument (Lab India) was used and data were collected at a 1 nm min<sup>-1</sup> scan rate.

### Synthesis of tetraethyl octane-1,1,8,8-tetracarboxylate (TEOC)

Diethyl malonate (20.0 g, 125.0 mmol), 1,6-dibromohexane (7.6 g, 31.3 mmol) and anhydrous potassium carbonate (25.8 g, 186.9 mmol) were added to 150 mL acetonitrile and the mixture was allowed to reflux for 18 h. The reaction mixture was cooled to room temperature, the solvent was evaporated and the residue was poured into water. The product was extracted with ethyl acetate. The organic fraction was washed with water two times and dried over anhydrous sodium sulphate. Excess diethyl malonate was removed under low pressure conditions at 140 °C. <sup>1</sup>H NMR (400 MHz, CDCl<sub>3</sub>)  $\delta$  (ppm): 4.2 (q, 8H,  $-\text{OCH}_2-\text{CH}_3$ ), 3.3 (t, 2H,  $-\text{CH}(\text{COO})_2-$ ), 1.8



(m, 4H,  $-\text{CH}_2-\text{CH}_2-$ ), 1.3 (m, 4H,  $-\text{CH}_2-\text{CH}_2-\text{CH}_2-$ ), 1.1 (t, 12H,  $-\text{CH}_3$ ).  $^{13}\text{C}$  NMR (100 MHz,  $\text{CDCl}_3$ )  $\delta$  (ppm): 169.8 ( $-\text{COO}-$ ), 61.3 ( $-\text{O}-\text{CH}_2-$ ), 52.3 ( $-\text{CH}-(\text{COO})_2$ ), 29.0 ( $-\text{CH}_2-$ ), 27.4 ( $-\text{CH}_2-$ ), 13.9 ( $-\text{CH}_3$ ). FTIR ( $\text{cm}^{-1}$ ): 786 (m, C-H), 860 (s, C-H), 1175 (s, C-O), 1729 (s,  $-\text{COO}-$ ), 2860 (m, C-H), 2935 (m, C-H).

### Synthesis of butyl hexylmalonate (BHM)

$\alpha$ -Butyl diethylmalonate (BEM, 0.5 g, 2.3 mmol) and *n*-hexanol (0.9 g, 9.2 mmol) were taken in a round-bottomed flask and 5 mol% of  $\text{Sn}(\text{Oct})_2$  (46.8 mg, 0.11 mmol) with respect to BEM was added to the above mixture at 140 °C. The reaction was carried out under solvent-free conditions for 5 h. The product was directly used for characterization without any further purification.  $^1\text{H}$  NMR (400 MHz,  $\text{CDCl}_3$ )  $\delta$  (ppm): 4.1 (q, 4H,  $-\text{COOCH}_2\text{CH}_2-$ ), 3.3 (t, 2H,  $-\text{CH}(\text{COO})_2-$ ), 1.9 (m, 6H,  $-\text{CH}_2-\text{CH}_2-\text{CH}-$ ), 1.6 (m, 12H,  $-\text{COOCH}_2\text{CH}_2-$ ), 1.3 (m, 4H,  $-\text{CH}_2-\text{CH}_2-\text{CH}_2-$ ), 0.9 (t, 9H,  $-\text{CH}_3$ ).  $^{13}\text{C}$  NMR (100 MHz,  $\text{CDCl}_3$ )  $\delta$  (ppm): 169.8 ( $-\text{COO}-$ ), 65.6 ( $-(\text{COO})_2-\text{CH}_2-\text{CH}_2-$ ), 52.2 ( $-\text{CH}-(\text{COO})_2$ ), 31.40 ( $-\text{CH}_2-\text{CH}_2-$ ), 28.6 ( $-\text{CH}_2-\text{CH}_2-$ ), 25.7 ( $-\text{CH}_2-\text{CH}_2-$ ), 22.4 ( $-\text{CH}_2-\text{CH}_3$ ), 13.9 ( $-\text{CH}_3$ ). FTIR ( $\text{cm}^{-1}$ ): 796 (s, C-H), 890 (s, C-H), 1157 (s, C-O), 1734 (s,  $-\text{COO}-$ ), 2860 (m, C-H), 2931 (m, C-H), HRMS (ESI-TOF)  $m/z$ :  $[\text{M} + \text{H}]$  calculated for  $[\text{C}_{19}\text{H}_{36}\text{O}_4] = 329.2693$ . Found 329.2681.

### Synthesis of TEOC-based CANs

TEOC (2.0 g, 5.0 mmol), PTE (0.8 g, 6.0 mmol) and  $\text{Sn}(\text{Oct})_2$  (0.2 g, 10 mol% with respect to TEOC) were taken in a round-bottomed flask and heated at 140 °C for 8 h. Then the mixture was poured into a Teflon Petri dish and kept for 12 h in a vacuum oven at 140 °C for curing purposes.

### Degradation and reprocessing of the CANs

Small pieces of the CANs (5.0 g) were taken in a round bottomed flask with *n*-butanol (20 mL) and refluxed at 120 °C for 15 h. The strips dissolved and a homogeneous solution was obtained. Subsequently, the solvent was evaporated and the mass was incubated at 140 °C for 12 h in a vacuum oven for reformation of the networks.

### Swelling ratio of the samples

Different CAN (TEOC-PTE, TEOC-TEA, TEOC-PTMO, and TEOC-PTMO-PTE) films (100 mg) were immersed in organic solvents, *e.g.* toluene, octanol, acetone, DMF, methanol and water. The weight gain was measured after different time intervals by a gravimetric method till saturation. The swelling ratio was calculated using the following equation:

$$\text{Weight Swelling Ratio} = \frac{\text{Final Weight} - \text{Initial Weight}}{\text{Initial Weight}} \times 100\%$$

### Separation of toluene from azeotropic mixtures with CANs

Binary (toluene : methanol = 1.15 : 0.38, vol : vol) and ternary azeotropes (toluene : methanol : water = 1.15 : 0.19 : 0.06, vol : vol) were prepared by following reported procedures.<sup>55,56</sup> A TEOC-PTMO-PTE strip (200 mg) was dipped in the above azeo-

tropic mixture. The strip was removed after regular time intervals and the peak absorbance at 260 nm in the UV-Vis spectra of the azeotropic mixture was monitored to determine the concentration of toluene.

To examine the reusability of the CAN films, the soaked TEOC-PTMO-PTE film was heated at 110 °C for 1 h to evaporate the solvent. The dry TEOC-PTMO-PTE film was again dipped in a fresh azeotropic mixture and the toluene absorption efficiency was monitored. The above process was carried out for five consecutive cycles of soaking and drying.

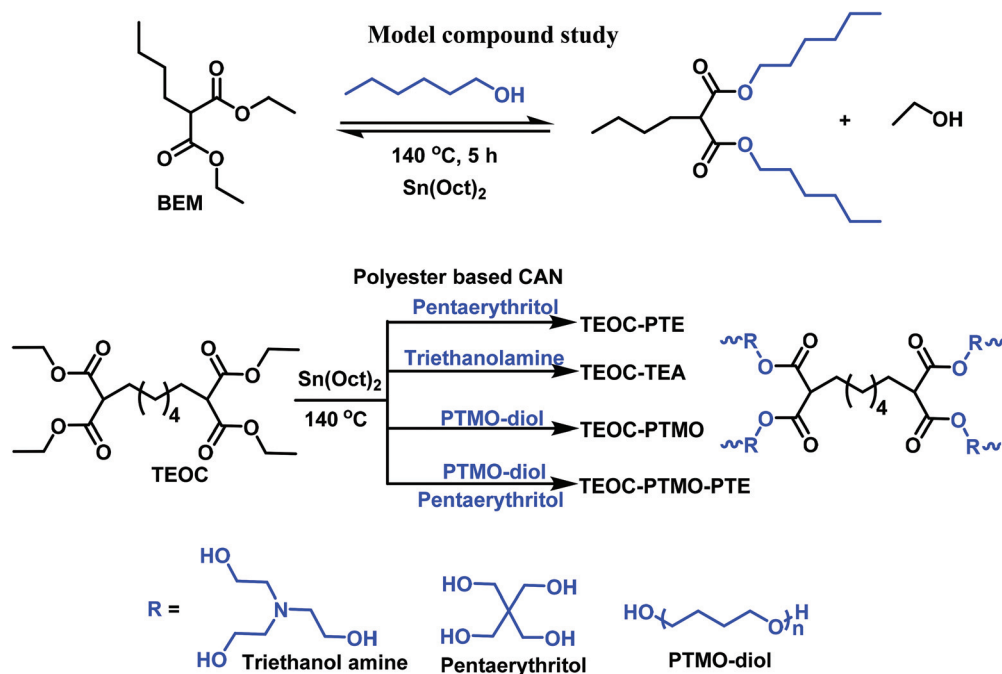
## Results and discussion

### Study of model compounds

BEM possessing structural similarity to the polymerizable tetraester (TEOC) was chosen as the model compound and the rate of trans-esterification with *n*-hexanol was studied in the presence of  $\text{Sn}(\text{Oct})_2$  (Scheme 1). At 140 °C, the trans-esterification reaction reached equilibrium within 2 h in the presence of 5 mol%  $\text{Sn}(\text{Oct})_2$  under solvent-free conditions. In  $^1\text{H}$  NMR spectra, the intensity of the quartet at 4.2 ppm for  $-\text{COOCH}_2\text{CH}_3$  gradually decreased and new multiplets at 4.1 and 1.6 ppm accountable to  $-\text{COOCH}_2\text{CH}_2-$  and  $-\text{COOCH}_2\text{CH}_2-$  of the product appeared, suggesting the successful exchange of the ethoxy moiety with the *n*-hexyloxy group in BEM (Fig. 1A and B). Similarly, a new peak at 65.6 ppm accountable to  $-\text{COOCH}_2\text{CH}_2-$  appeared and the peak at 61 ppm for  $-\text{COOCH}_2\text{CH}_3$  in BEM disappeared, supporting the conversion (Fig. 1C). The principal peak at 329.2681 ( $\text{M} + \text{H}$ ) accountable to the exchanged product (BHM) was observed in HRMS spectra (Fig. S1, ESI†). The conversion of the above trans-esterification was monitored under different temperature conditions (110–140 °C) until equilibrium. The half-lives ( $t_{1/2}$ ) of the above reactions were used to determine the rate constant ( $k$ ) using a second-order rate equation. The  $k$  values were subsequently plotted against the temperature to construct an Arrhenius plot and determine the activation energy ( $E_a$ ) of the reaction (Fig. 2). The  $E_a$  value of the trans-esterification reaction between  $\alpha$ -alkyl substituted  $\beta,\beta'$ -diesters and primary alcohols was around  $157.8 \pm 4.8 \text{ kJ mol}^{-1}$ .

### Synthesis of polyester-based CANs

On the basis of the model compound study, the CANs were synthesized at 140 °C with adequate  $\text{Sn}(\text{Oct})_2$  (10 mol% with respect to TEOC) loading. Four different CANs were synthesized using TEOC and three different multi-ols. The molar compositions of TEOC and multi-ols were optimized based on their tensile properties (Table S1, ESI†). The molar ratio of TEOC : PTE = 5 : 6 (mol : mol) was used to prepare the TEOC-PTE CAN. Similarly, the other CANs were synthesised using a suitable molar ratio of TEOC to the multi-ol (Table 1). The CANs were colored and were mostly transparent in nature (Fig. 3B). The mechanical and thermal properties of the CANs were measured (Table 2). UTS and  $E$  values were obtained in



**Scheme 1** Trans-esterification of the model compound and synthesis of polyester-based CANs using TEOC and different multi-ols.

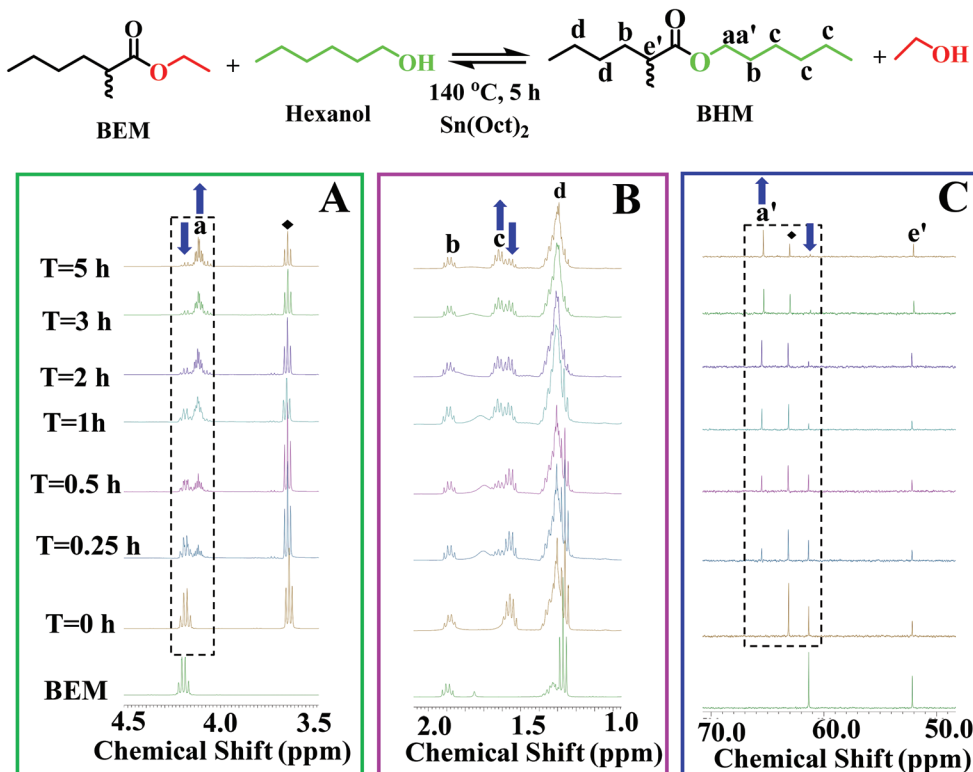


**Fig. 1** (A and B)  $^1\text{H}$  NMR and (C)  $^{13}\text{C}$  NMR spectra of the precursor and reaction mixture recorded at different time intervals. The reaction of BEM and *n*-hexanol was conducted in the presence of  $\text{Sn}(\text{Oct})_2$  at  $140^\circ\text{C}$ . The peak marked with “♦” represents the amount of *n*-hexanol present in the reaction mixture. The schematic on the top of the figure shows the exchange of the ethoxy moiety with the *n*-hexyloxy group in the ester.

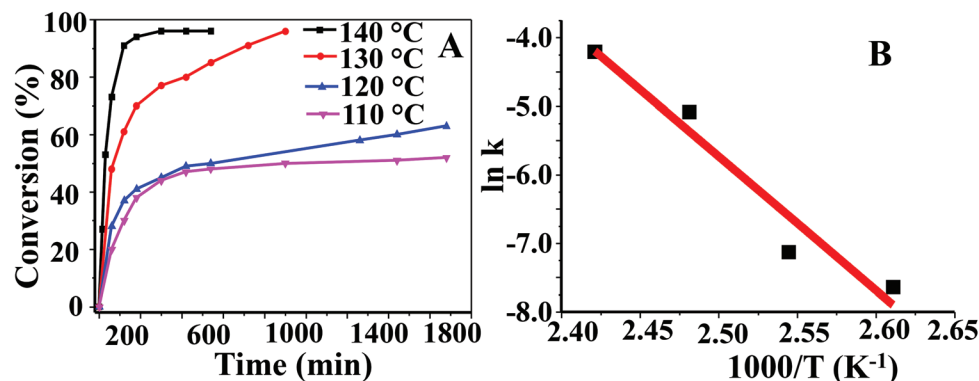


Fig. 2 (A) The conversion plots of the trans-esterification of BEM with *n*-hexanol at 140 °C, 130 °C, 120 °C and 110 °C. The ratio between BEM and *n*-hexanol was 1 : 4 (mol : mol) for the trans-esterification reaction. (B) The Arrhenius plot of the trans-esterification reaction is constructed by plotting the  $t_{1/2}$  values under different temperature conditions using second-order kinetics.

Table 1 Composition and nomenclature of CANs

Code <sup>b</sup>	Multi-ol	TEOC (mmol)	Multi-ol (mmol)
TEOC-PTE	PTE	4.97	5.96
TEOC-TEA	TEA	4.97	5.97
TEOC-PTMO	PTMO	4.97	2.76
TEOC-PTMO-PTE <sup>a</sup>	PTMO/PTE	4.97	6.00

<sup>a</sup> PTMO : PTE = 1.2 : 4.8 (mmol : mmol). <sup>b</sup> 10 mol% of Sn(Oct)<sub>2</sub> with respect to TEOC was used in all the cases and the reaction temperature was 140 °C.

the range of 0.1–1.1 MPa and 0.7–1.8 MPa, respectively. The CANs synthesized using a mixture of PTMO and PTE exhibited a UTS value of 1.1 MPa and elongation at break ( $\epsilon$ ) values up to 301%.

The CANs based on PTMO and TEOC exhibited a maximum  $\epsilon$  value of 595%. The storage modulus ( $E'$ ) values of the CANs were obtained in the range of 0.8–4.9 MPa. The  $E'$  values were higher than the loss modulus ( $E''$ ) values in all the cases, supporting the crosslinked nature of the sample (Fig. 3D).<sup>57</sup> The DMTA plots of the CANs revealed that the  $E'$  values were

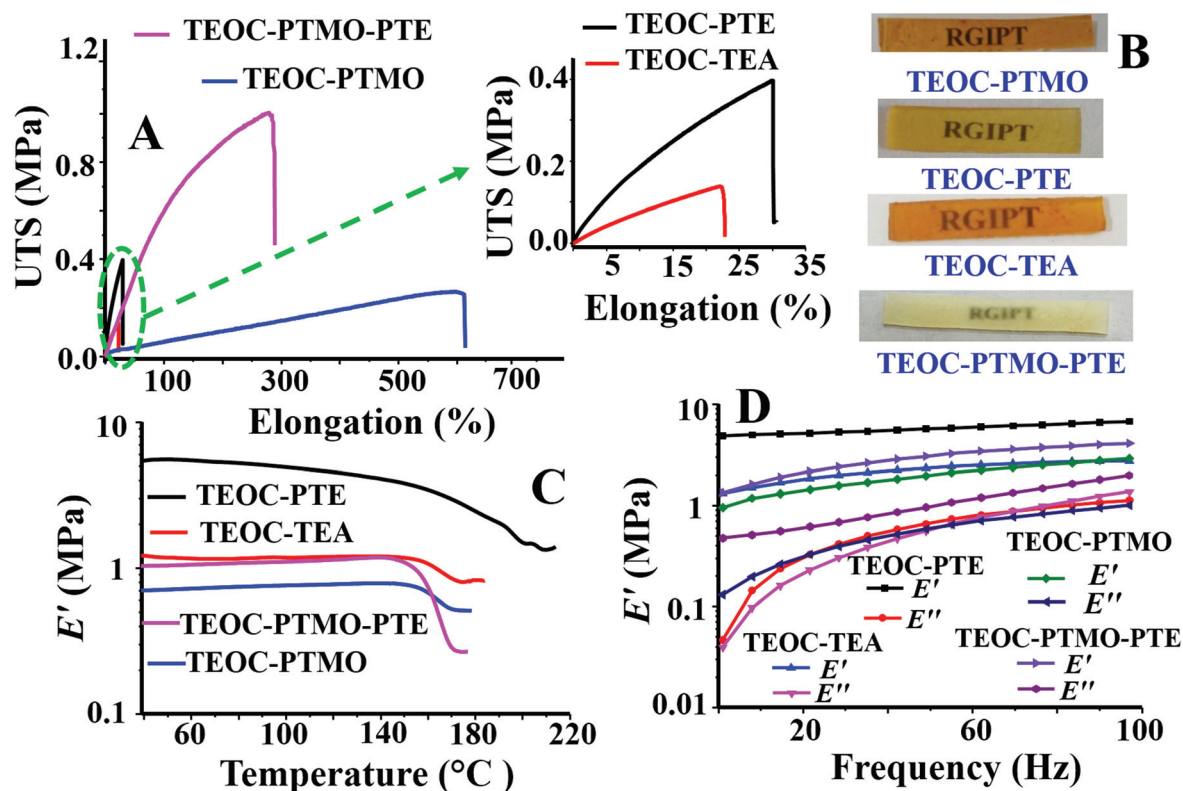


Fig. 3 (A) Tensile plots of the CANs, (B) photographs of different CAN films, (C) DMTA traces and (D) the frequency sweep plots of the CANs.

**Table 2** Mechanical and thermal properties of the CANs

CANs	UTS <sup>a</sup> (MPa)	$\epsilon^a$ (%)	$E^a$ (MPa)	TGA <sup>c</sup> (°C)	$E''^b$ (MPa)	$d_c \times 10^3$ (mol cm <sup>-3</sup> )
TEOC-PTE	0.5 ± 0.06	30.0 ± 3.0	1.8 ± 0.04	215	4.9 ± 0.4	0.13 ± 0.06
TEOC-TEA	0.1 ± 0.01	23.0 ± 3.0	1.1 ± 0.01	205	1.2 ± 0.1	0.07 ± 0.04
TEOC-PTMO	0.3 ± 0.06	595.0 ± 15.0	0.8 ± 0.01	200	0.8 ± 0.1	0.05 ± 0.02
TEOC-PTMO-PTE	1.1 ± 0.03	301.3 ± 22.0	0.7 ± 0.03	210	1.1 ± 0.1	0.03 ± 0.01

<sup>a</sup> From tensile analysis, the UTS, elongation at break ( $\epsilon$ ) and  $E$  values were calculated. <sup>b</sup> The values were obtained from DMTA analysis.

<sup>c</sup> Represents the onset of decomposition in TGA measurement.

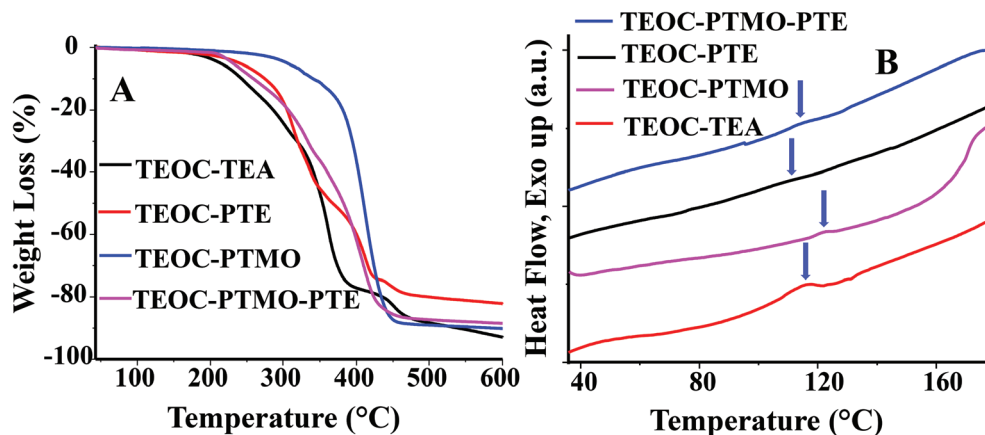


**Fig. 4** (A) TGA traces of different CANs. (B) The second heating DSC traces of different CANs recorded under a N<sub>2</sub> atmosphere.

retained up to 140 °C under thermomechanical conditions. A sharp decline in the  $E'$  value occurred on increasing the temperature beyond 140 °C, suggesting the onset of the relaxation of the CANs. Interestingly, small exothermic humps were noticed in the temperature range of 120–140 °C in the DSC spectra of all CANs (Fig. 4B). Both the DMA and DSC data suggested that the relaxation temperature of the CANs may be in the range of 120–140 °C. The crosslink density ( $d_c$ ) values of the CANs were determined from the plateau modulus data at temperatures in the range of 168–201 °C. The values were obtained in the range of  $0.03 \times 10^{-3}$  to  $0.13 \times 10^{-3}$  mol cm<sup>-3</sup>. Only the CAN (TEOC-PTMO-PTE) synthesized using PTMO and PTE exhibited stress relaxation behavior and the  $E_a$  value ( $145.0 \text{ kJ mol}^{-1}$ ) calculated from the corresponding Arrhenius plot was similar to that from the model compound study (Fig. S2, ESI†). However, the other networks failed to show stress relaxation characteristics, which may be attributed to the unavailability of free -OH groups in these CANs and the absence of a possible trans-esterification exchange reaction.

The CANs showed thermal stability above 200 °C and the onset of weight loss in TGA traces was observed at ~215 °C (Table 2, Fig. 4A). The maximum weight loss occurred between 300 and 420 °C. Polyesters are known to degrade above 300 °C from the literature.<sup>58</sup> The stability of these CANs was monitored in acidic and basic solutions. The CAN films were dipped in acidic and basic media for 12 h at room temperature. The films were subsequently removed, dried and subjected to tensile measurement. The tensile plots of the recovered films were similar to those of the pristine films (Fig. 5A).

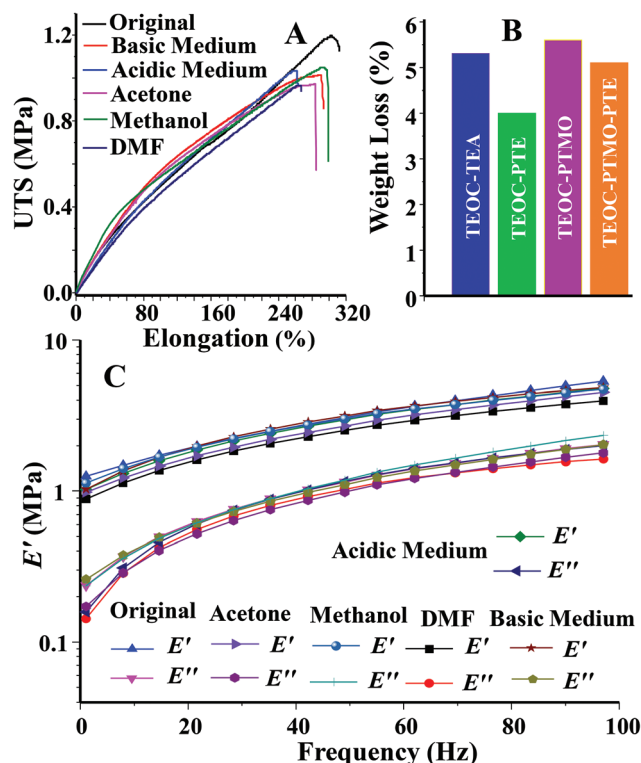


**Fig. 5** (A) Tensile data of the original sample and the samples after removal from acidic and basic solutions, acetone, methanol, and DMF after 12 h, (B) weight loss data of different CANs in the DMF solvent, and (C) frequency sweep data of the original sample and the samples after removal from acidic and basic solutions, acetone, methanol and DMF after 12 h.



Similarly,  $E'$  versus frequency plots were comparable to those of the original CAN films and  $E'$  values of acid- and base-treated films were observed in the range of 1.0–1.2 MPa (Fig. 5C). The weight loss of different CANs in DMF was below 6% after 12 h of dipping under ambient conditions (Fig. 5B). In other solvents such as acetone, THF and methanol, the weight loss was limited to 4% only. The UTS values of the solvent-processed samples were in the range of 0.9–1.1 MPa. The above data suggested that these CAN samples possess adequate solvent tolerance.

### Solution reprocessability of the CANs

These CANs were anticipated to depolymerize in alcoholic solvents *via* competitive trans-esterification reaction under moderate temperature conditions. Small pieces of TEOC-PTMO-PTE were taken in a round-bottomed flask and the mixture was refluxed at 120 °C in *n*-butanol for 15 h. The films readily dissolved in the solvent, suggesting depolymerisation of the sample (Fig. 6A2 and B2). The samples kept in

other non-alcoholic solvents remained intact under similar conditions after 15 h (Fig. S3, ESI†). The homogeneous solution of TEOC-PTMO-PTE obtained in *n*-butanol was placed at 140 °C under reduced pressure conditions to gradually evaporate the solvent and initiate the crosslinking process. The samples re-formed after 12 h under the above conditions. The UTS ( $\sim 1.0$  MPa) and  $E'$  ( $\sim 0.61$  MPa) values of the 1<sup>st</sup> reprocessed sample of TEOC-PTMO-PTE were comparable to those of the original sample (UTS  $\sim 1.1$  MPa and  $E' \sim 0.7$  MPa). The tensile properties of the 2<sup>nd</sup> reprocessed sample (UTS =  $\sim 0.9$  MPa and  $E' = \sim 0.5$  MPa) also retained up to 90% of the original properties, suggesting that the solution processability of these CANs *via* reactive depolymerisation is effective (Fig. 6C and Table S2, ESI†).

### Separation of aromatics from azeotropic mixtures

Polyether-based networks are known to absorb various organic solvents and exhibit organogel characteristics.<sup>59</sup> Therefore, CANs were prepared by adding PTMO along with PTE to

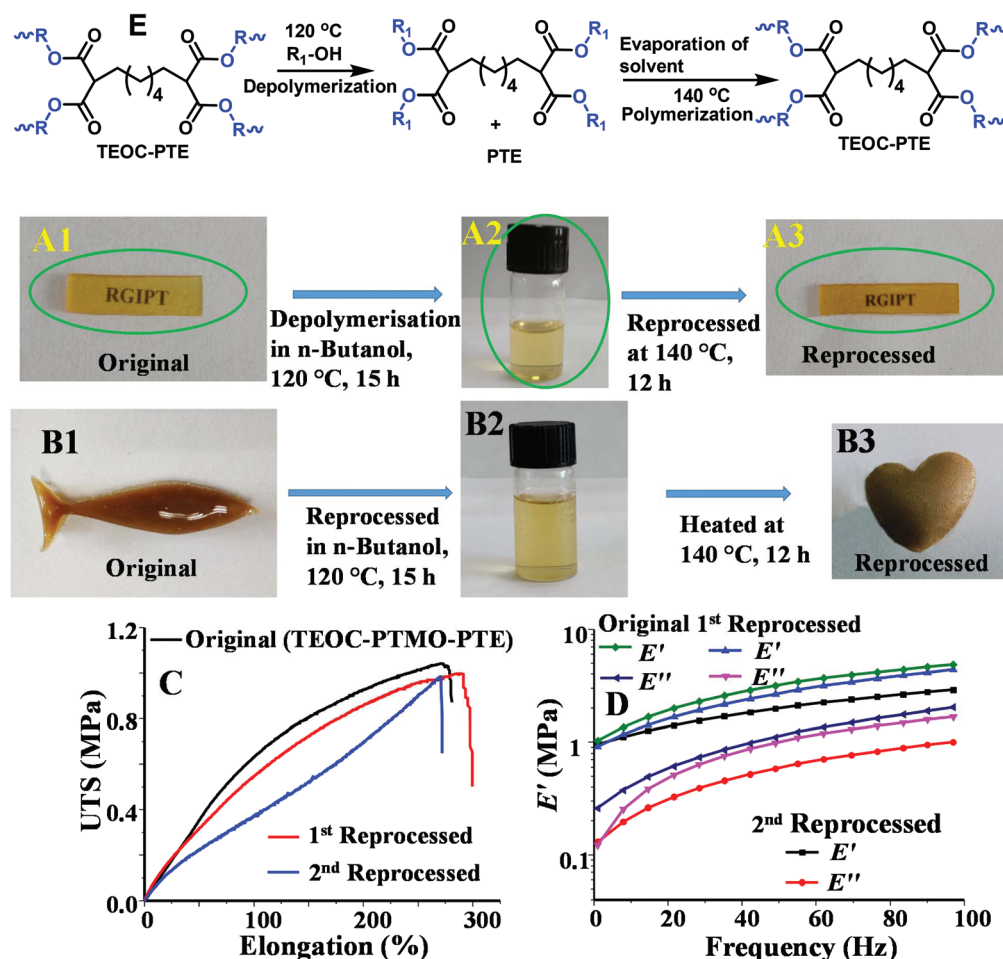


**Fig. 6** (A1) The as-prepared TEOC-PTE film, (A2) homogeneous solution in *n*-butanol after depolymerization, (A3) re-formed TEOC-PTE from the depolymerized solution, (B1) photograph of original TEOC-PTMO-PTE, (B2) the sample after depolymerization, (B3) the reprocessed sample of TEOC-PTMO-PTE, (C) tensile plots of the original, 1<sup>st</sup> and 2<sup>nd</sup> reprocessed samples, (D) frequency sweep plots of the as-prepared, 1<sup>st</sup> and 2<sup>nd</sup> reprocessed samples, and (E) the scheme showing the degradation of TEOC-PTE *via* competitive trans-esterification with the solvent and re-formation on the evaporation of the solvent.



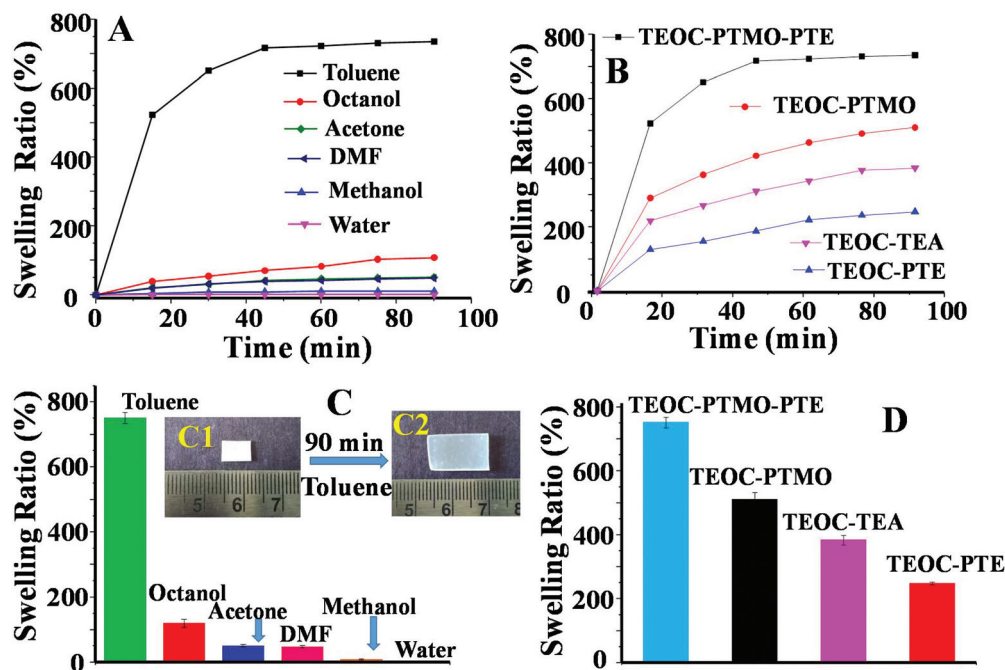


Fig. 7 (A) Swelling ratio of TEOC-PTMO-PTE in various organic solvents and water after regular time intervals, (B) swelling ratio of different CANs in toluene after regular time intervals, (C) maximum swelling ratios of TEOC-PTMO-PTE in different solvents and (D) maximum swelling ratios of different CANs in toluene. The inset in (C) shows dry- and toluene-soaked TEOC-PTMO-PTE after 90 min in toluene.

induce organogel ability in the CANs. The capacity of these CANs to absorb organic solvents was evaluated by dipping a thin strip of TEOC-PTMO-PTE in different organic solvents under ambient conditions. Interestingly, the CAN selectively absorbed toluene compared to a range of other organic solvents (Fig. 7A).

The weight swelling ratio value of TEOC-PTMO-PTE was 750% in toluene, whereas the values were less than 120% in other organic solvents. However, the swelling ratio values of other CANs were  $\leq 500\%$  in toluene (Fig. 7B). The swelling was relatively fast and equilibrium was reached within 1 h of dipping in the solvent (Fig. 7B). The above data suggested that the CANs may be utilized to separate toluene from different

organic and azeotropic mixtures. Separation of azeotropic mixtures is an important problem in industries and requires cumbersome process units such as pressure-swing distillation, extractive distillation and critical temperature and pressure conditions.<sup>60,61</sup>

Binary (toluene:methanol = 1.15:0.38, vol:vol) and ternary (toluene:methanol:water = 1.15:0.19:0.06, vol:vol) azeotropes were prepared and the efficiency of TEOC-PTMO-PTE to remove toluene from the above azeotropic mixtures was assessed. Strips of TEOC-PTMO-PTE were dipped in the above azeotropic mixtures for a fixed time period. The strips were removed and UV-Visible spectra of the mixture were recorded after specific time intervals. The peak at 260 nm

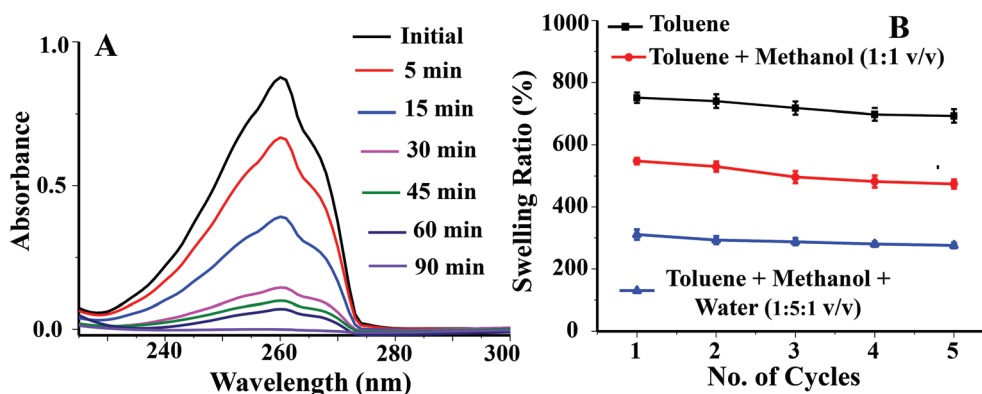


Fig. 8 (A) Removal of toluene from a methanol-toluene azeotrope (1.15:0.38, vol:vol) by TEOC-PTMO-PTE, (B) swelling ratio of TEOC-PTMO-PTE in toluene, toluene:methanol (1:1, vol/vol) and toluene:methanol:water (1:5:1, vol/vol) in repetitive cycles.

assigned to toluene gradually decreased with the immersion time. The peak disappeared within 90 min, suggesting the maximum removal of toluene from the mixture (Fig. 8A and S4, ESI†).

The reusability of these CANs was assessed by repeatedly using a set of TEOC-PTMO-PTE strips for five continuous absorption-desorption cycles in toluene and different solvent mixtures. The sample retained up to 90% swelling ratio till the 5<sup>th</sup> cycle (Fig. 8B). The fast absorption and reusability of the samples suggested that these CANs may be a cost effective and convenient alternative to be used in large-scale fixed beds for continuous separation of azeotropic mixtures.

## Conclusions

$\alpha$ -Substituted  $\beta,\beta'$ -diesters undergo trans-esterification reaction under moderate temperature conditions (110 to 140 °C) in the presence of a minor amount of Sn(Oct)<sub>2</sub>. This trans-esterification chemistry is suitable for synthesizing solution processable and recyclable CANs. Typical volatile alcohols swiftly depolymerize the CANs *via* competitive trans-esterification. Evaporation of the solvent and subsequent heating are sufficient to re-form the CANs with comparable properties to those of the original samples. Overall, the synthesis and reprocessability of these CANs are convenient and cost-effective. Organogels can be designed and synthesized by incorporating suitable polyether diols into the CANs. The PTMO-based CANs are capable of selectively absorbing aromatics among several organic solvents and separating toluene from various azeotropic mixtures. These CANs are promising for use in fixed bed columns for the continuous separation of aromatics from azeotropic mixtures in the future.

## Conflicts of interest

The authors declare no competing financial interest.

## Acknowledgements

S. D. is thankful to the CSIR, India, for providing a Senior Research Fellowship (09/1201(0002)/19-EMR-I). The authors acknowledge DST-SERB (EMR/2016/006464), India, for financial support.

## References

- M. M. Obadia, A. Jourdain, P. Cassagnau, D. Montarnal and E. Drockenmuller, *Adv. Funct. Mater.*, 2017, **27**, 1703258.
- W. Zou, J. Dong, Y. Luo, Q. Zhao and T. Xie, *Adv. Mater.*, 2017, **29**, 1606100.
- Z. Wang, X. Lu, S. Sun, C. Yu and H. Xia, *J. Mater. Chem. B*, 2019, **7**, 4876–4926.
- Q. Li, S. Ma, S. Wang, W. Yuan, X. Xu, B. Wang, K. Huang and J. Zhu, *J. Mater. Chem. A*, 2019, **7**, 18039–18049.
- H. Zhang, C. Cai, W. Liu, D. Li, J. Zhang, N. Zhao and J. Xu, *Sci. Rep.*, 2017, **7**, 11833.
- R. Mo, J. Hu, H. Huang, X. Sheng and X. Zhang, *J. Mater. Chem. A*, 2019, **7**, 3031–3038.
- M. Guerre, C. Taplan, R. Nicolay, J. M. Winne and F. E. Du Prez, *J. Am. Chem. Soc.*, 2018, **140**, 13272–13284.
- H. A. Houck, E. Blasco, F. E. Du Prez and C. Barner-kowollik, *J. Am. Chem. Soc.*, 2019, **141**, 12329–12327.
- A. Chao, I. Negulescu and D. Zhang, *Macromolecules*, 2016, **49**, 6277–6284.
- C. M. Hamel, X. Kuang, K. Chen and H. J. Qi, *Macromolecules*, 2019, **52**, 3636–3645.
- P. Chakma and D. Konkolewicz, *Angew. Chem., Int. Ed.*, 2019, **58**, 9682–9695.
- M. M. Obadia, B. P. Mudraboyina, A. Serghei, D. Montarnal and E. Drockenmuller, *J. Am. Chem. Soc.*, 2015, **137**, 6078–6083.
- M. Bednarek and P. Kubisaa, *Polym. Chem*, 2019, **10**, 1848–1872.
- F. Sordo, S. Mougner, N. Loureiro, F. Tournilhac and V. Michaud, *Macromolecules*, 2015, **48**, 4394–4402.
- W. Denissen, J. M. Winne and F. E. Du Prez, *Chem. Sci.*, 2016, **7**, 30–38.
- N. Zheng, J. Hou, Y. Xu, Z. Fang, W. Zou, Q. Zhao and T. Xie, *ACS Macro Lett.*, 2017, **6**, 326–330.
- Z. Wang, L. Guo, H. Xiao, H. Cong and S. Wang, *Mater. Horiz.*, 2020, **7**, 282–288.
- S. Xiang, Q. Hua, P. Zhao, W. Gong, C. Li and M. Zhu, *Chem. Mater.*, 2019, **31**, 5081–5088.
- R. Mafi, S. M. Mirabedini, M. M. Attar and S. Moradian, *Prog. Org. Coat.*, 2005, **54**, 164–169.
- L. M. Polgar, M. Van Duin, A. A. Broekhuis and F. Picchioni, *Macromolecules*, 2015, **48**, 7096–7105.
- A. Chao, I. Negulescu and D. Zhang, *Macromolecules*, 2016, **49**, 6277–6284.
- S. Debnath, R. R. Ujjwal and U. Ojha, *Macromolecules*, 2018, **51**, 9961–9973.
- R. Baruah, A. Kumar, R. R. Ujjwal, S. Kedia, A. Ranjan and U. Ojha, *Macromolecules*, 2016, **49**, 7814–7824.
- A. Dirksen, S. Dirksen, T. M. Hackeng and P. E. Dawson, *J. Am. Chem. Soc.*, 2006, **128**, 15602–15603.
- K. Kim, H. J. Cho, J. Lee, S. Ha, S. G. Song, S. Kim, W. S. Yun, S. K. Kim, J. Huh and C. Song, *Macromolecules*, 2018, **51**, 8278–8285.
- A. Biswas, V. K. Aswal, P. U. Sastry, D. Rana and P. Maiti, *Macromolecules*, 2016, **49**, 4889–4897.
- X. Chen, L. Li and J. M. Torkelson, *Polymer*, 2019, **178**, 121604.
- B. M. Matysiak, P. Nowak, I. Cvrtila, C. G. Pappas, B. Liu and S. Otto, *J. Am. Chem. Soc.*, 2017, **139**, 6744–6751.
- W. Denissen, M. Driesbeke, R. Nicolay, L. Leibler, J. M. Winne and F. E. Du Prez, *Nat. Commun.*, 2017, **8**, 14857.
- R. L. Snyder, D. J. Fortman, G. X. De Hoe, M. A. Hillmyer and W. R. Dichtel, *Macromolecules*, 2018, **51**, 389–397.

- 31 M. F. Dunn, T. Wei, R. N. Zuckermann and T. F. Scott, *Polym. Chem.*, 2019, **10**, 2337–2343.
- 32 P. R. Christensen, A. M. Scheuermann, K. E. Loeffler and B. A. Helms, *Nat. Chem.*, 2019, **11**, 442–448.
- 33 J. E. Richards and D. Philp, *Chem. Commun.*, 2016, **52**, 4995–4998.
- 34 C. Urata, R. Hönes, T. Sato, H. Kakiuchida, Y. Matsuo and A. Hozumi, *Adv. Mater. Interfaces*, 2019, **6**, 1801358.
- 35 Y. Chen, W. Wang, D. Wu, H. Zeng, D. G. Hall and R. Narain, *ACS Appl. Mater. Interfaces*, 2019, **11**, 44742–44750.
- 36 A. Sidorenko, T. Krupenkin, A. Taylor, P. Fratzl and J. Aizenberg, *Science*, 2007, **315**, 487–490.
- 37 T. Yuan, X. Qu, X. Cui and J. Sun, *ACS Appl. Mater. Interfaces*, 2019, **11**, 32346–32353.
- 38 L. Yue, S. Wang, V. Wulf and I. Willner, *Nat. Commun.*, 2019, **10**, 4774.
- 39 M. Fevre, G. O. Jones, M. Zhang, J. M. García and J. L. Hedrick, *Adv. Mater.*, 2015, **27**, 4714–4718.
- 40 H. L. Lim, J. C. Chuang, T. Tran, A. Aung, G. Arya and S. Varghese, *Adv. Funct. Mater.*, 2011, **21**, 55–63.
- 41 L. Shi, Y. Zeng, Y. Zhao, B. Yang, D. Ossipov, C. Tai, J. Dai and C. Xu, *ACS Appl. Mater. Interfaces*, 2019, **11**, 46233–46240.
- 42 S. Xia, Q. Zhang, S. Song, L. Duan and G. Gao, *Chem. Mater.*, 2019, **31**, 9522–9531.
- 43 Z. Li, F. Zhou, Z. Li, S. Lin, L. Chen, L. Liu and Y. Chen, *ACS Appl. Mater. Interfaces*, 2018, **10**, 25194–25202.
- 44 C. H. Fox, G. M. ter Hurne, R. J. Wojtecki, G. O. Jones, H. W. Horn, E. W. Meijer, C. W. Frank, J. L. Hedrick and J. M. García, *Nat. Commun.*, 2015, **6**, 7417.
- 45 J. V. Accardo and J. A. Kalow, *Chem. Sci.*, 2018, **9**, 5987–5993.
- 46 H. Wang and Y. Cheng, *Mater. Chem. Front.*, 2019, **3**, 472–475.
- 47 Y. Gao, W. Liu and S. Zhu, *Macromolecules*, 2018, **51**, 8956–8963.
- 48 H. Song, Z. Fang, B. Jin, P. Pan, Q. Zhao and T. Xie, *ACS Macro Lett.*, 2019, **8**, 682–686.
- 49 A. Demongeot, R. Groote, H. Goossens, T. Hoeks and L. Leibler, *Macromolecules*, 2017, **50**, 6117–6127.
- 50 Y. Yu, G. Storti and M. Morbidelli, *Ind. Eng. Chem. Res.*, 2011, **50**, 7927–7940.
- 51 L. Self, N. D. Dolinski, M. S. Zayas, J. R. De Alaniz and C. M. Bates, *ACS Macro Lett.*, 2018, **7**, 817–821.
- 52 O. R. Cromwell, J. Chung and Z. Guan, *J. Am. Chem. Soc.*, 2015, **137**, 6492–6495.
- 53 Y. Li, O. Rios, J. K. Keum, J. Chen and M. R. Kessler, *ACS Appl. Mater. Interfaces*, 2016, **8**, 15750–15757.
- 54 S. Debnath, S. Kaushal and U. Ojha, *ACS Appl. Polym. Mater.*, 2020, DOI: 10.1021/acsapm.0c00016.
- 55 Y. Li and C. Xu, *Ind. Eng. Chem. Res.*, 2017, **56**, 4017–4037.
- 56 A. Yang, R. Wei, S. Sun, S. Wei, W. Shen and I. Chien, *Ind. Eng. Chem. Res.*, 2018, **57**, 8036–8056.
- 57 D. Wang, J. Xu, J. Chen, P. Hu, Y. Wang, W. Jiang and J. Fu, *Adv. Funct. Mater.*, 2020, **30**, 1907109.
- 58 S. V. Mankar, M. N. G. Gonzalez, N. Warlin, N. Valsange, N. Rehnberg, S. Lundmark, P. Jannasch and B. Zhang, *ACS Sustainable Chem. Eng.*, 2019, **7**, 19090–19103.
- 59 X. Zhang, Z. Li, X. Che, L. Yu, W. Jia, R. Shen, J. Chen, Y. Ma and G. Q. Chen, *Biomacromolecules*, 2019, **20**, 3303–3312.
- 60 W. Li, L. Shi, B. Yu, M. Xia, J. Luo, H. Shi and C. Xu, *Ind. Eng. Chem. Res.*, 2013, **52**(23), 7836–7853.
- 61 J. A. Jaime, G. Rodríguez and I. D. Gil, *Ind. Eng. Chem. Res.*, 2018, **57**(29), 9615–9626.